Carbohydrate Polymers 220 (2019) 141–148

Contents lists available at ScienceDirect

Carbohydrate Polymers

journal homepage: www.elsevier.com/locate/carbpol

Removal of pharmaceuticals by novel magnetic genipin-crosslinked chitosan/graphene oxide-SO_3H composite

Yangshuo Liu[a,*], Rong Liu[a], Ming Li[a], Fucheng Yu[b], Chiyang He[a]

[a] Hubei Key Laboratory of Biomass Fibers and Eco-Textile Chemistry, Wuhan 430073, China
[b] School of Material Science and Engineering, Lanzhou University of Technology, China

ARTICLE INFO

Keywords:
Water treatment
Ibuprofen
Tetracycline
Chitosan/graphene oxide-SO_3H
Adsorption

ABSTRACT

A novel magnetic adsorbent genipin-crosslinked chitosan/graphene oxide-SO_3H (GC/MGO-SO_3H) composite was prepared and used as adsorbents of environmental pollutant. The GC/MGO-SO_3H exhibit typical superparamagnetic behavior. The adsorption characteristics of GC/MGO-SO_3H composite to pharmaceuticals were investigated through batch experiments. The maximum adsorption capacity of ibuprofen and tetracycline increases from 113.27 to 138.16 mg/g and 473.25 to 556.28 mg/g with the increase in temperature from 298 to 313 K. The adsorption kinetics and isotherms were investigated in detail to reveal that the kinetics and equilibrium adsorptions are well described by pseudo-second-order kinetic and Freundlich isotherm model, respectively. This study has demonstrated that the GC/MGO-SO_3H composite could be utilized as an efficient and with high speed.

1. Introduction

Pharmaceuticals have been worldwide used in the treatment of human and animal diseases. However, large amounts of pharmaceuticals wastewater are produced (Kaeseberg et al., 2018). The complex aromatic molecular structures and xenobiotic properties of pharmaceutical pollutants, which make them difficult to degrade (Nachiappan & Gopinath, 2015). Pharmaceutical pollutants have several effects on human beings, animals and the environment (Frieke Kuper et al., 2015). It is very necessary to remove these pharmaceutical pollutants from environment.

During the last three decades, study on removal of pharmaceutical pollutants in wastewater by several physical, chemical, biological and photochemical approaches have been reported. Among these methods, absorption is regarded as an easy, high efficiency and economic process as it can be used to remove different types of coloring materials (Rafatullah, Sulaiman, Hashim, & Ahmad, 2010; Regti et al., 2016). Various adsorbents, such as activated carbon, natural materials, bio-adsorbents, waste materials, modified expanded graphite (Zhao & Liu, 2009), and carbon nanotube (Kang, Yu, Ge, Xiao, & Xu, 2017) have been studied for adsorption from aqueous solutions and some of them expressed good organic pollutants adsorption property.

Recently, magnetic adsorbents have emerged as effective adsorbents for environmental decontamination since magnetic separation simply involves applying an external magnetic field to extract the adsorbents (Han, Li, Wang, & Chen, 2015; Lan, Leng, Guo, Wu, & Gan, 2014; Reddy & Yun, 2016; Su, Ye, & Hmidi, 2017; Wang et al., 2009).

Chitosan magnetic composite, with high saturation magnetization and magnetic permeability (Iordache et al., 2018). Graphene and graphene-based functional materials have caused increasing interests in adsorption capacity due to its large surface area (Fan et al., 2011; Gao et al., 2011; Liu, Chung, Oh, & Seo, 2012). It has been used for the adsorption methyl violet, orange-G, rhodamine-B and express good adsorption property (Wu, Yang, Liu, Tan, & Xiao, 2018). Chitosan magnetic composite have been widely used in high frequency power applications (Iordache et al., 2018; Sargin, Arslan, & Kaya, 2019), The chitosan magnetic composite system is known to possess good magnetic properties (Alizadeh, Delnavaz, & Shakeri, 2018; Tabaraki & Sadeghinejad, 2018; Wang et al., 2019). It has been reported that the salts of chitosan magnetic composite could integrate with graphene oxide (GO) by the electrostatic interaction (Shah, Jan, & Tasmia, 2018).

Many magnetic adsorbents based on graphene have been used for remove pharmaceuticals and metal ions from aqueous solutions (Fu, Wang, Liu, & Zeng, 2014; Li, Zhang, & Xuan, 2015; Li et al., 2018; Naeimi & Faghihian, 2018). The sulfo group is known to form stable complexes with various pharmaceuticals. The chitosan magnetic composite was usually used genipin to improve its mechanical stability over a wider pH range (Gorgieva, Vuherer, & Kokol, 2018).

* Corresponding author.
E-mail address: liuyangshuo8858@163.com (Y. Liu).

https://doi.org/10.1016/j.carbpol.2019.05.060
Received 2 February 2019; Received in revised form 5 May 2019; Accepted 21 May 2019
Available online 24 May 2019

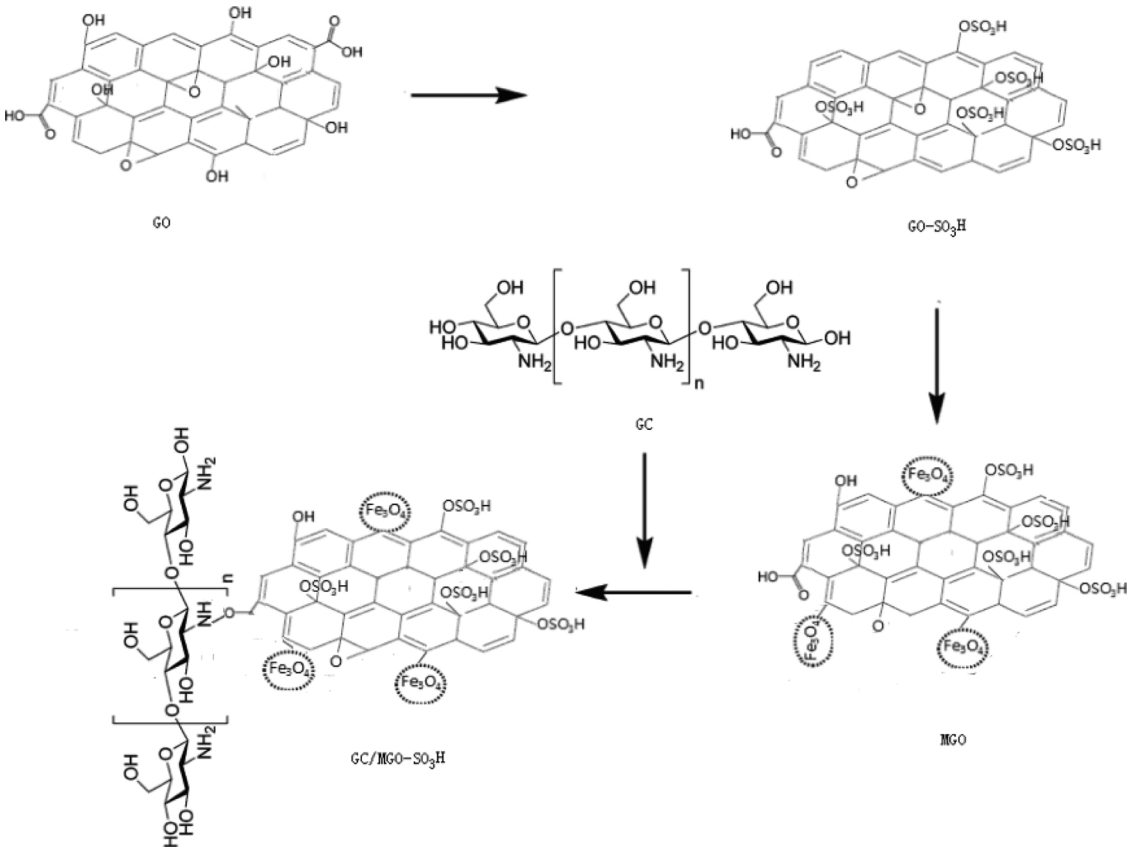

Scheme 1. Synthesis procedure of GC/MGO-SO_3H.

In this paper, we demonstrate a hybrid formed by FeCo/Graphene oxide with its three-dimensional nanostructures as environmental pollutant by utilizing the microporous structure with ultralarge surface area for adsorption of ibuprofen and tetracycline from aqueous solution. Kinetic study, adsorption mechanism, and thermodynamic analysis on the pharmaceutical adsorption were investigated.

2. Materials and methods

2.1. Materials

Ibuprofen, sodium borohydride, tetracycline, genipin and chitosan (medium molecular weight, 200 < viscosity < 800 cP, 1% in 1% acetic acid) were purchased from Sigma-Aldrich. *N*-hydroxysuccinimide (NHS), 1-ethyl-3-(3-dimethylaminopropyl) carbodiimide hydrochloride (EDC), $FeSO_4{\cdot}7H_2O$ and $FeCl_3{\cdot}6H_2O$ were purchased from Aldrich Chemical Co.. Natural flake graphite used to prepare GO was provided by Sinopharm Chemical Reagent Co. Ltd. GO was prepared by oxidation of natural graphite powder according to a modified Hummers' method (Hummers & Offeman, 1958; Xu et al., 2009).

2.2. Preparation of GC/MGO-SO_3H

Preparation of GO-SO_3H and GO-SO_3H@Fe_3O_4 according to a modified Liu' method (Liu, Li, & He, 2017). In brief, The reaction of covalent attachment between the carboxylic groups of GO and amine of sulfanilic acid can be prepared as follows: NHS (1.71 g) and EDC (2.85 g) were added to 50 mL of GO (10 mg/mL) solution and then the mixture was stirred at 0 °C for 2 h.0.5 g SA was added to the obtained mixture and stirred overnight atroom temperature and the solution color changed gradually frompale yellow to grayish. The obtained GO-SO_3H was washed and dispersed in water and then stored at room temperature for further ruse. Chitosan (0.4 g) was dissolved in 20 mL acetic acid (2% w/v) and sonicated for 2 h. Next, genipin (1 wt%) were added followed by drop wise addition. Then the mixture was mechanically stirred for 1.0 h at room temperature to allow the carboxyl groups on the GO to become activated. Finally, the product was collected using an external magnet, then washed three times with distilled water. 20 mL of the homogeneous GO-SO_3H dispersion (0.5 mg/mL) was mixed with 20 mL of GC aqueous solution. The carboxyl group of GO chemically reacts with the amine group of chitosan with consequent formation of a chemical bond between GO and magnetic chitosan. The mixtures were put in a water bath at 50∘C for 12 h. Then laboratory freeze dryer at -50∘C (Christ Germany) to produce the aerogel of GC/GO-SO_3H. The whole process of GC/GO-SO_3H aerogel preparation is shown in Scheme 1.

2.3. Characterization of GC/MGO-SO_3H

The morphologies and microstructure of GC/MGO-SO_3H nanocomposite were used to characterize by scanning electron microscopy (SEM, JEM-1010, Jeol, Tokyo, Japan). Magnetic hysteresis loop were obtained by using JDM-13 vibrating sample magnetometer.

2.4. Determination of the adsorption of Ibuprofen and tetracycline onto GC/MGO-SO_3H

Typically, 5 mg of GC/MGO-SO_3H was added in 100 mL of tetracycline or/and ibuprofen solution with the desired initial concentration (20–200 mg/L or 1–10 mg/L), and then the mixture was stirred at 25∘C with a stirring speed of 200 rpm.

To investigate the effect of pH on adsorption of pharmaceutical, the pH range of 2–12 was used. The acidity of pharmaceutical solutions was adjusted with HNO_3 and NaOH prior to test. The GC/MGO-SO_3H was mixed with 20 mL of ibuprofen (100 mg/L, pH 7) and tetracycline (400 mg/L, pH 7) and shaken at 298 K. Samples were collected at 3 h

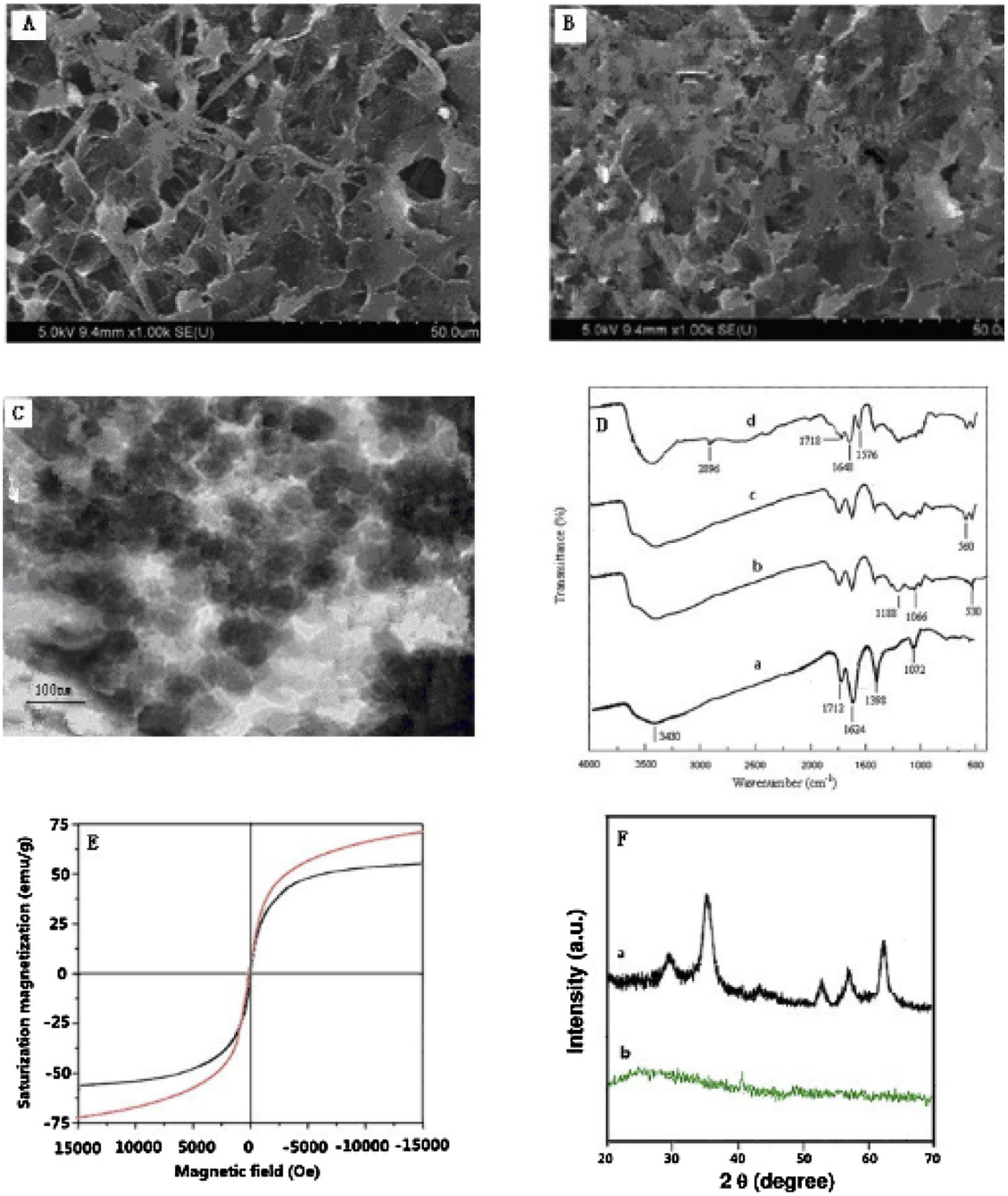

Fig. 1. Morphological characterization (A) SEM image, (B) SEM image of GC/MGO-SO3H after adsorption of pharmaceutical, (C) TEM image of GC/MGO-SO_3H, (D) FT-IR images of (a) GO, (b) GO-SO_3H, (c) MGO-SO_3H and (d) GC/MGO-SO_3H, (E) magnetization curves for Fe_3O_4, and GC/MGO-SO_3H hybrid and (F) XRD patterns of (a) GC/MGO-SO_3H and (b) GO.

for pharmaceutical concentration and adsorption capacity (Qe) determinations.

To evaluate the thermodynamic properties, these samples were shaken at 298, 313 and 323 K, respectively.

The adsorbed amount of organic pollutants was measured with a UV–vis (Varian, Cary50) spectrophotometer at appropriate wave lengths corresponding to the maximum absorption peak of each organic pollutant, 364 nm for tetracycline and 220 nm for ibuprofen.

2.5. Desorption and reuse of GC/MGO-SO_3H

GC/MGO-SO_3H with adsorbed ibuprofen and tetracycline were stirred in 0.1or 0.01 M NaOH solution for 2 h at 298 K. Then, the obtained GC/MGO-SO_3H was recovered by filtration and dried in a vacuum oven at 50∘C before further use.

3. Results and discussion

3.1. Characterization

Fig. 1(A and B) presents the SEM micrograph of the surface of GC/MGO-SO_3H nanocomposites. Fig.1(A) shows that the GC/MGO-SO_3H sponge was well assembled and interconnected with pore size of 0.2–1.0 of micrometers and the Fe_3O_4 nanoparticles were successfully assembled on the surface of GC/MGO-SO_3H. Fig.1(B) shows that after the adsorption of pharmaceutical with the GC/MGO-SO_3H, the surface

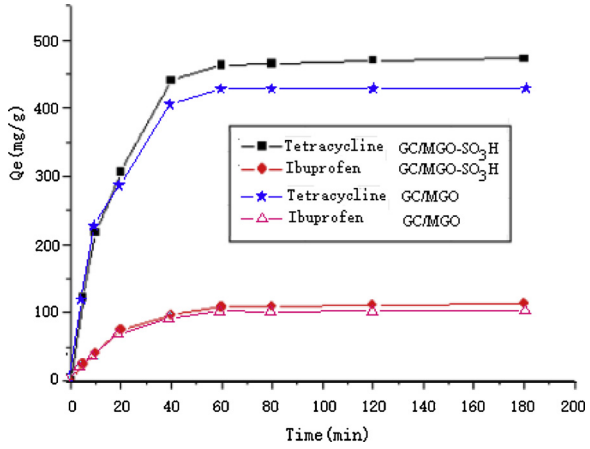

Fig. 2. Effect of contact time on ibuprofen and tetracycline absorption onto GC/MGO and GC/MGO-SO_3H.

morphology of the GC/MGO-SO_3H has changed significantly, the pharmaceutical has been loaded on the surface of the GC/MGO-SO_3H.

Representative TEM images of the obtained GC/MGO-SO_3H hybrids are show in Fig. 1(C). It can be seen that Fe_3O_4 have been covered on the GC/MGO-SO_3H surface. Those particles are of spherelike morphology in general, and the diameter of those particles is ranging between 80 and 90 nm.

Fig. 1(D) shows the FTIR spectra of GO, GO-SO_3H, MGO-SO_3H, GC/MGO-SO_3H. GO has shown absorption peaks at 3430 cm^{-1}, 1732 cm^{-1}, 1624 cm^{-1}, 1398 cm^{-1} and 1048 cm^{-1} relating to O—H stretching vibrations, C═O stretching vibrations in carboxyl groups, stretching vibration of aromatic C═C bond, and C–O alkoxy vibrations, respectively. 1188, 1066 and 530 cm^{-1} are the sulfo group -SO_3H expansion and contraction absorption peak. The MGO-SO_3H spectrum contained a band at 560 cm^{-1} that was not found in the chitosan spectrum. This peak was assigned to Fe-O (Wen et al., 2015), and its presence showed that MGO-SO_3H had been successfully synthesized. The peaks at 1718 and 1648 cm^{-1} were absent in the FT-IR spectrum of GC/MGO-SO_3H, which indicates the hydrogen bonding between chitosan and GO. The results implied the existence of the interaction between chitosan and GO. The magnetization curve of GC/MGO-SO_3H hybrid was measured at 298 K. Fig. 1E shows the magnetization hysteresis loop of the as-prepared GC/MGO-SO_3H in the presence and absence of GC-GO-SO_3H, suggesting that GC/MGO-SO_3H exhibit typical superparamagnetic behavior. The saturation magnetization intensity of GC/MGO-SO_3H was 55.4 emu g^{-1}, which is sufficient for magnetic separation from solution with a conventional magnet.

The XRD pattern of GC/MGO-SO_3H is shown in Fig. 1(F). From the spectrum, the intense diffraction peaks at the Bragg angles 2θ of 30.09∘, 35.44∘,37.15∘, 43.05∘, 53.29∘, 56.96∘ and 62.51∘correspond to the (220), (311), (222), (400), (422), (511) and (440) facets of the cubic spinel crystal structure of Fe_3O_4, respectively, which match well with the data of magnetite (JCPDS File no. 19-0629) (Hou, Zhang, Zhu, Li, & Wang, 2011). The broad diffraction peaks are indications of the nanoparticles with very small sizes.

3.2. Effect of contact time

Several adsorption demonstrations have been reported. The O-carboxymethyl-Nlaurylchitosan/γ-Fe_2O_3 (OCh-LM) has great adsorption capacity of ibuprofen. The maximum adsorption capacities of the adsorbents were found to be 99 mg/g at 25 °C and pH 7.0 (Chahm & Rodrigues, 2017). Yu et al. coupled small amount of Fe_3O_4 with GO to prepare magnetic graphene oxide sponge (MGOS) for the adsorption of tetracycline with a high capacity of 473 mg/g, showing 50% increase comparing to GO (Yu et al., 2017). The maximum adsorption capacities of magnetic graphene oxide (MGO) were 252 mg/g for tetracycline was reported by Huang et al. (Huang et al., 2019). The low adsorption capacity of

(Graphene oxide functionalized magnetic Nanoparticles) GO-MPs, 39.1, 45.0 and 42.6 mg/g for tetracycline (TC) (Oxytetracycline) OTC and (Chlortetracycline) CTC, respectively, was ascribed to the low specific surface area and less interactions of Fe_3O_4 with the pollutants (Jin, Wang, Sun, Ai, & Wang, 2015). Four background cations (Na^+, K^+, $Ca^{2+}$and Mg^{2+}) with a concentration of 0.01 M showed little influence on the tetracycline adsorption at the studied pH range while the divalent heavy metal cation Cu(II) could significantly enhance the adsorption. The results indicated that the highest adsorption capacity of tetracycline were 183.47 mmol/kg and 67.57 mmol/kg on Fe_3O_4@SiO_2-Chitosan/GO (MSCG) with and without Cu (II), respectively. (Huang et al., 2017)

Fig. 2 shows the effect of contact times on the adsorption of ibuprofen and tetracycline on GC/MGO-SO_3H. The adsorption capacity has a remarkable increase with a treatment duration of 120 min, then stayed almost constantly.

There were initially a larger number of vacant sites on adsorbent for binding the pharmaceuticals. With further increase in time, many vacant sites were bound to pharmaceuticals, resulting the repulsive forces between the pharmaceuticals and the adsorbent.

3.3. Effect of concentration

The adsorption capacities of tetracycline onto GC/MGO-SO_3H were studied at various initial tetracycline concentrations (20, 50, 100 and 200 mg/L). As shown in Fig. 3, results indicated that adsorption capacities of tetracycline increased with a corresponding increase in initial concentrations (20–200 mg/L). The maximum being attained with an initial tetracycline concentrations of 200 mg/L. The adsorption

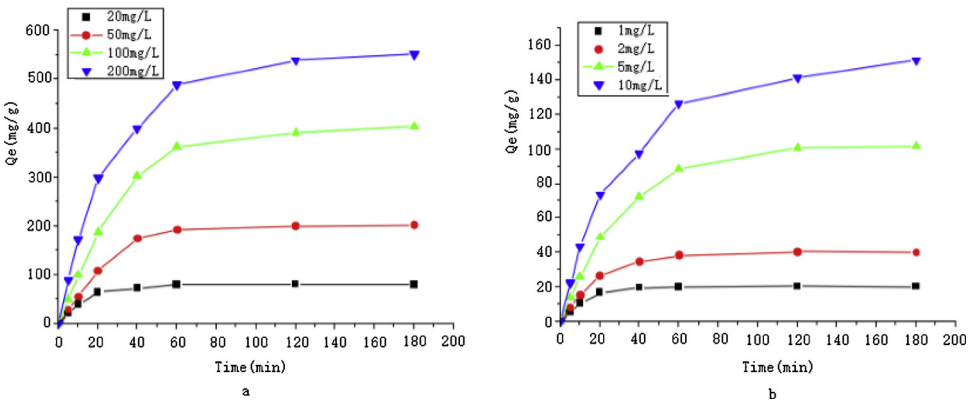

Fig. 3. Effect of initial concentration on ibuprofen and tetracycline absorption onto GC/MGO-SO_3H.

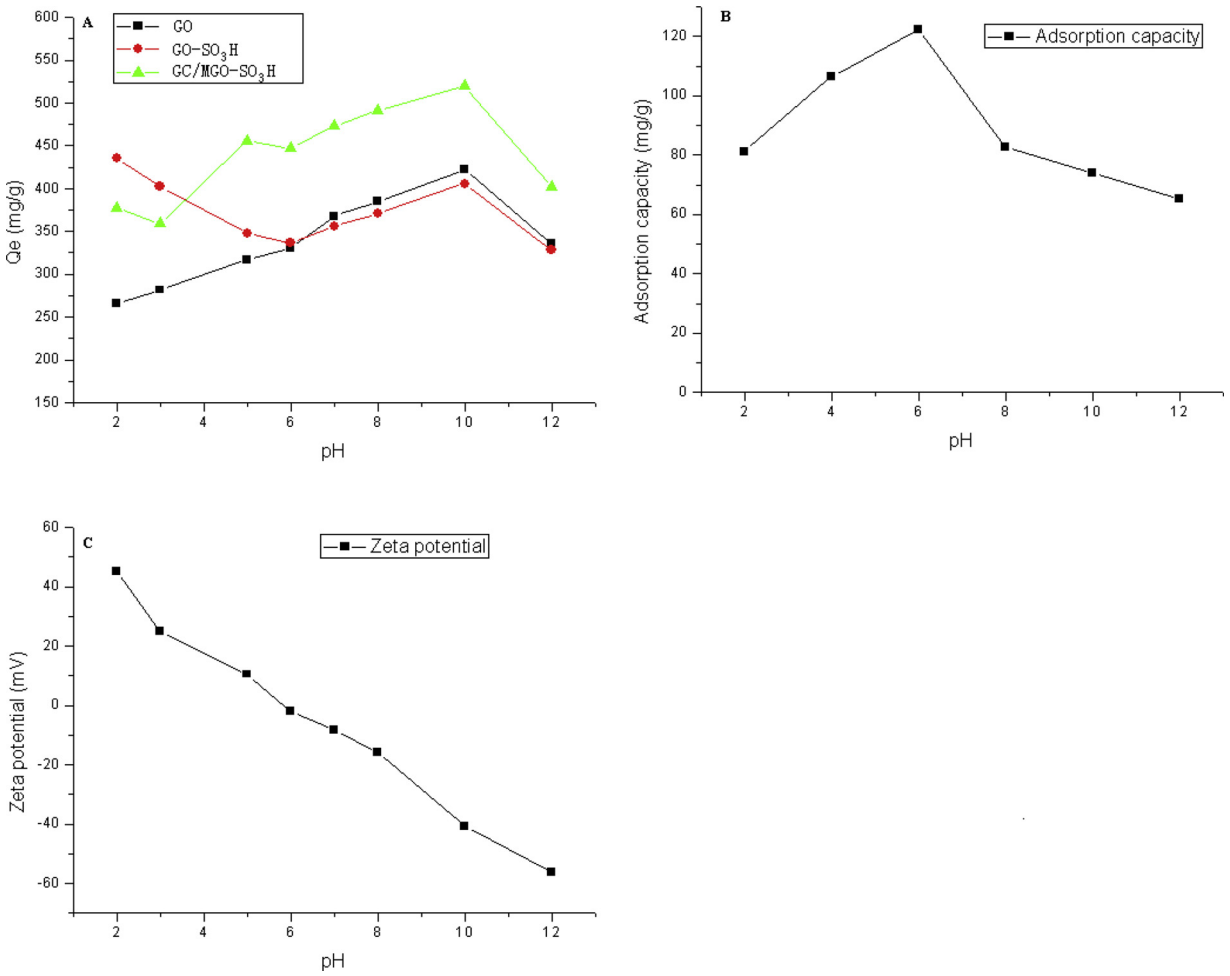

Fig. 4. Effect of pH, (A) the adsorption of tetracycline using GO, GO-SO_3H and GC/MGO-SO_3H, (B) the adsorption of ibuprofen using GC/MGO-SO_3H, (C) the zeta potential.

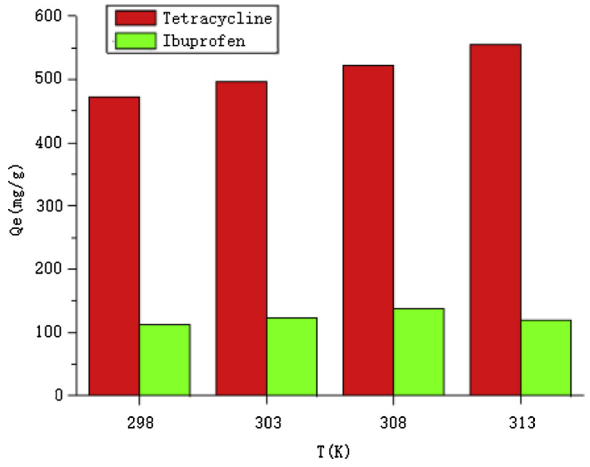

Fig. 5. The amount of ibuprofen and tetracycline adsorbed by GC/MGO-SO_3H at equilibrium state at.298–313 K.

capacities of ibuprofen onto GC/MGO-SO_3H were studied at various initial ibuprofen concentrations (1, 2.5, 5 and 10 mg/L). The adsorption capacity increased from 19.92 to 150.28 mg/g when the initial ibuprofen concentration increased from 1 to 10 mg/L. Obviously, the initial concentration played an important role in the adsorption of ibuprofen and tetracycline by GC/MGO-SO_3H.

3.4. Effect of pH value on adsorption

The influence of pH on the adsorption capacity for ibuprofen and tetracycline by GC/MGO-SO_3H was carried out in the pH value to 2, 3, 5, 6, 7, 8, 10 and 12 using acid/base buffer solutions. For tetracycline, the molecule charge changed at different pH ranges. As shown in Fig. 4, with the increase of pH, the adsorption capacity increased gradually. The maximum adsorption capacity was obtained at pH 10. The capacity of adsorption thereafter slightly decreased. For GC/MGO-SO_3H, where the increase of pH led to the GO surface becomes abundant with negatively charged functional groups. The ionic interaction would be reinforced to bind the tetracycline molecules on surface. In addition, At very high pH, both tetracycline and GC/MGO-SO_3H were negatively charged, thus the electrostatic repulsion occurred between charges. Therefore, in the middle pH range of solution, the adsorption lead to a higher capacity. For GO-SO_3H, the adsorption capacity of tetracycline was seen to decrease as solution pH values increased from 2 to 6. The capacity of adsorption thereafter increased. For GC/GO-SO_3H, the phenomenon was similar with GO-SO_3H. Fig. 4B shows the removal of ibuprofen was seen to increase from 65.42 to 122.35 as solution pH values increased from 2 to 6. At pH higher than 6, ibuprofen became negative. These negative charges might have been involved in electrostatic interactions with the surrounding ibuprofen ions and became stronger with rise in pH values therefore resulting in a corresponding decrease in adsorption capacity of ibuprofen.

As shown in Fig. 4(C), the zeta potential of GC/MGO-SO_3H was negative at pH values from 2.0 to 12.0. Tetracycline is an organic

Table 1
Pseudo-first order and pseudo-second order rate parameters for the adsorption of tetracycline and ibuprofen on GC/MGO-SO_3H.

Pharmaceuticals	Temp	Q_{exp}(mg/g)	Pseudo-first order kinetic			Pseudo-second order kinetic		
			K_1	Q_c(mg/g)	R^2	K_2	Q_c(mg/g)	R^2
Tetracycline	298	421.28	0.4262	436.80	0.9489	0.002007	442.21	0.9983
	308	474.62	0.5623	483.27	0.9245	0.003122	483.34	0.9992
	313	492.71	0.3234	495.64	0.9128	0.001821	499.27	0.9978
Ibuprofen	298	126.38	0.4925	127.82	0.9567	0.002101	129.34	0.9982
	308	158.77	0.5026	159.38	0.9423	0.004388	160.22	0.9927
	313	140.14	0.4628	142.23	0.9546	0.001984	145.27	0.9934

Table 2
Parameters for the calculation of Langmuir and Freundlich Models.

Pharmaceuticals	Temp	Langmuir			Freundlich		
		K_L	Q_m(mg/g)	R^2	K_F	1/n	R^2
Tetracycline	298	2.001	460.12	0.9998	16.63	0.6446	0.8776
	308	1.683	492.75	0.9982	17.86	0.6837	0.8938
	313	2.346	500.68	0.9995	17.98	0.5872	0.9026
Ibuprofen	298	2.017	138.62	0.9999	5.46	1.2530	0.9122
	308	2.236	160.83	0.9992	6.35	1.1263	0.8247
	313	1.865	146.27	0.9978	5.68	1.2724	0.7893

compound with a pKa_1 of 7.8 and pKa_2 of 9.6, the molecule charge changed at different pH ranges. When pH was lower than 3.3, tetracycline was positive molecules. At pH 3.3–7.8, tetracycline was zwitterion and nearly neutral. At pH higher than 7.8, tetracycline became negative. At low pH, the electrostatic interaction should be weak, because the protonation of −OH/−COOH on GC/MGO-SO_3H, making GC/MGO-SO_3H less negative. At very high pH, both tetracycline and GC/MGO-SO_3H were negatively charged, thus the electrostatic repulsion occurred. Therefore, only in the middle pH range, the adsorption reached high capacity. Ibuprofen shows similar phenomena. The pKa of ibuprofen is 4.5. The adsorption capacity of ibuprofen was seen to increase from 65.42 to 122.35 as solution pH values increased from 2 to 6. At pH higher than 6, ibuprofen became negative. These negative charges might have been involved in electrostatic interactions with the surrounding ibuprofen ions and became stronger with rise in pH values therefore resulting in a corresponding decrease in adsorption capacity of ibuprofen.

Results may be explained by sulfonic acid group and chitosan. At pH < pHpzc, the GC/MGO-SO_3H surfaces are positively charged due to the protonation reactions:

$$\text{-C–OH} + H^+ \text{ —— -C-}OH_2{}^+$$

$$\text{-C-}SO_3H + H^+ \text{ —— -C-}SO_3H_2{}^+$$

$$\text{-C–}NH_2 + H^+ \text{ —— -C-}NH_3{}^+$$

whereas at pH > pHpzc, the GC/MGO-SO_3H surfaces are negatively charged because of the deprotonation reactions:

$$\text{-C–OH} + H^+ \text{ —— -C–}O^- + H^+$$

$$\text{-C-}SO_3H + H^+ \text{ —— -C-}SO_3{}^- + H^+$$

At low pH, the electrostatic interaction should be weak, because the protonation of -C-SO_3H, −OH, −COOH, -NH_2 on GC/MGO-SO_3H, making GC/MGO-SO_3H less negative. At very high pH, both tetracycline and GC/MGO-SO_3H were negatively charged, thus the electrostatic repulsion occurred.

3.5. Effect of temperature

The influence of temperature on the adsorption of tetracycline by GC/MGO-SO_3H was investigated. As shown in Fig. 5, for tetracycline, higher temperature resulted in higher adsorption capacity. This indicated that the adsorption of tetracycline on GC/MGO-SO_3H was endothermic in nature, which was consistent with most adsorption cases on graphene adsorbents.

The effect of temperature on adsorption of ibuprofen and tetracycline onto GC/MGO-SO_3H were investigated at 298 to 313 K. For tetracycline, It can be found that the adsorption capacity increases with the increment of temperature. The maximum adsorption capacity increases from 473.25 to 556.28 mg/g with the increase in temperature from 298 to 313 K. The experimental results indicate that the adsorption process was endothermic and an improved adsorption capacity of GC/MGO-SO_3H for pharmaceutical pollutants at higher temperature. This can be ascribed to the better interaction between the pharmaceutical pollutants and the GC/MGO-SO_3H hybrids at enhanced temperature.

Therefore, the effect of temperature on ibuprofen adsorption by GC/MGO-SO_3H was investigated within the temperature range of 298 to 313 K. Fig. 5 shows the increase of ibuprofen with acorresponding rise

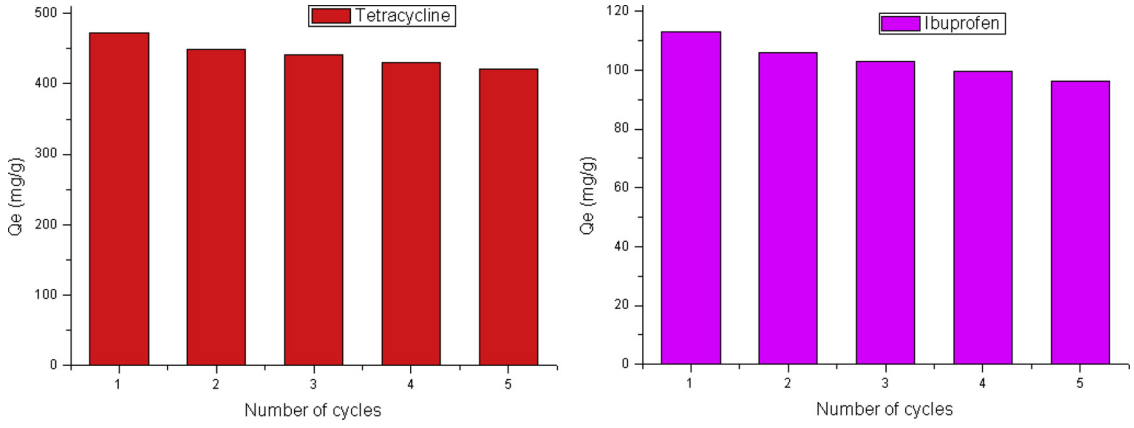

Fig. 6. The variation of adsorption capacity of GC/MGO-SO_3H using the recycled sample.

Table 3
The number of regeneration cycles for the adsorption of tetracycline and ibuprofen on GC/GO-SO_3H.

Pharmaceuticals	The number of regeneration cycles				
	1	2	3	4	5
Tetracycline	473.22	449.51	442.18	430.64	421.15
Ibuprofen	113.16	105.84	103.05	99.68	96.21

in temperature from 298 to 308 K, the highest occurring at 308 K. However, as the temperature of the system increases, the adsorption showed that a decline in the sorption process. The mechanisms of the adsorption process of ibuprofen on the GC/MGO-SO_3H were due to be the physical bonds between the ibuprofen molecules and the active site of the GC/MGO-SO_3H at that temperature.

The thermal energy allows the pharmaceutical pollutant adsorbate to diffuse across the external boundary layer and into the internal pores of the GC/MGO-SO_3H to enhance the quantity of adsorbed pharmaceutical pollutant molecules, resulting in the higher saturated equilibrium level. All above results show that the GC/MGO-SO_3H hybrids displayed the advantages of rapid adsorption rate, high adsorption capacity, and convenient magnetic separation for the removal of pharmaceutical pollutants in water.

3.6. Adsorption kinetics

The pharmaceuticals adsorption kinetics was investigated to verify the adsorption mechanism. The corresponding kinetic parameters for ibuprofen and tetracycline adsorption are given in Table 1. Based on the highest correlation coefficients ($R^2 > 0.99$), the adsorptions of ibuprofen and tetracycline were best described by the second-order kinetic equation. The theoretical Qe values for the adsorption of pharmaceutical pollutants on the GC/MGO-SO_3H were very close to the experimental Qe values in the case of second-order kinetics (Vadivelan & Kumar, 2005).

3.7. Evaluation of adsorption isotherm models

Langmuir and Freundlich adsorption isotherm models were used to determine the appropriate isotherm for ibuprofen and tetracycline adsorption on GC/MGO-SO_3H. Parameters of Langmuir and Freundlich models are shown in Table 2. According to the coefficients of determination, the Langmuir model fits better than Freundlich model. Therefore, this implies monolayer coverage of ibuprofen and tetracycline onto GC/MGO-SO_3H and also a homogeneous distribution of active sites on the adsorbent. The 1/n values of ibuprofen and tetracycline on the GC/MGO-SO_3H were 0.2414 and 0.2530, respectively, indicating that the pollutants could be easily to be adsorbed on the GC/MGO-SO_3H for the pharmaceutical pollutants.

3.8. Recycle and reuse of GC/MGO-SO_3H

Fig. 6 and Table 3 show the variation of the desorption percentages of GC/MGO-SO_3H after different cycles. It can be seen that the GC/MGO-SO_3H still maintained at least 85% adsorption capacity after 5 circulations. GC/MGO-SO_3H was eligible for the reliable adsorbent in the treatment of ibuprofen and tetracycline in the wastewater.

4. Conclusions

In this study, GC/MGO-SO_3H has been successfully fabricated. The GC/MGO-SO_3H acted as a good adsorbent to adsorb ibuprofen and tetracycline from wastewater. The adsorption of organic pollutants on GC/MGO-SO_3H is very fast process and can reach the adsorption equilibrium within 120 min. The adsorption kinetics of ibuprofen and tetracycline on the GC/MGO-SO_3H was investigated as a function of temperature, and pH. The adsorption isotherms agree well with the Freundlich model. Kinetic data were well fitted by a pseudo second-order model and consistent with an endothermic reaction. These results prove that the GC/MGO-SO_3H can be used as an effective adsorbent for the simple and rapid removal of ibuprofen and tetracycline from aqueous solutions.

Acknowledgments

This work was financially supported by the National Natural Science Foundation of China (51203125), and the Research Funds for the Hubei Key Laboratory of Biomass Fibers and Eco-Textile Chemistry (No. STRZ2018019)

Appendix A. Supplementary data

Supplementary material related to this article can be found, in the online version, at doi:https://doi.org/10.1016/j.carbpol.2019.05.060.

References

Alizadeh, B., Delnavaz, M., & Shakeri, A. (2018). Removal of Cd(II) and phenol using novel cross-linked magnetic EDTA/chitosan/TiO_2 nanocomposite. *Carbohydrate Polymers, 181*, 675–683.
Chahm, T., & Rodrigues, C. A. (2017). Removal of ibuprofen from aqueous solutions using O-carboxymethyl-Nlaurylchitosan/γ-Fe_2O_3. *Environmental Nanotechnology Monitoring & Management, 7*, 139–148.
Fan, Z., Kai, W., Yang, J., Wei, T., Zhi, L., Feng, J., et al. (2011). Facile synthesis of graphene nanosheets via Fe reduction of exfoliated graphite oxide. *ACS Nano, 5*, 191–198.
Frieke Kuper, C., Vogelsa, J., Kemmerling, J., Fehlert, E., Rühl-Fehlert, C., Vohr, H. W., et al. (2015). Integrated analysis of toxicity data of two pharmaceutical immunosuppressants and two environmental pollutants with immunomodulating properties to improve the understanding of side effects-A toxicopathologist's view. *European Journal of Pharmacology, 759*, 343–355.
Fu, Y., Wang, J. Y., Liu, Q. X., & Zeng, H. B. (2014). Water dispersible magnetic nanoparticle graphene oxide composites for selenium removal. *Carbon, 77*, 710–721.
Gao, W., Majumder, M., Alemany, L. B., Narayanan, T. N., Ibarra, M. A., Pradhan, B. K., et al. (2011). Engineered graphite oxide materials for application in water purification. *ACS Applied Materials & Interfaces, 3*, 1821–1826.
Gorgieva, S., Vuherer, T., & Kokol, V. (2018). Autofluorescence-aided assessment of integration and mu-structuring in chitosan/gelatin bilayer membranes with rapidly mineralized interface in relevance to guided tissue regeneration. *Materials Science & Engineering C, Materials for Biological Applications, 93*, 226–241.
Han, S., Li, X., Wang, Y., & Chen, S. N. (2015). Multifunctional imprinted polymers based on CdTe/CdS and magnetic graphene oxide for selective recognition and separation of p-t-octylphenol. *Chemical Engineering Journal, 271*, 87–95.
Hou, C. Y., Zhang, Q. H., Zhu, M. F., Li, Y. G., & Wang, H. Z. (2011). One-step synthesis ofmagnetically-functionalized reduced graphite sheets and their use inhydrogels. *Carbon, 49*, 47–53.
Huang, B. Y., Liu, Y. G., Li, B., Liud, S. B., Zeng, G. M., Zeng, Z. W., et al. (2017). Effect of Cu (II) ions on the enhancement of tetracycline adsorption by Fe_3O_4@SiO_2-Chitosan/graphene oxide nanocomposite. *Carbohydrate Polymers, 157*, 576–585.
Huang, D., Wu, J. Z., Wang, L., XingmeiLiu, X. M., Meng, J., Tang, X. J., et al. (2019). Novel insight into adsorption and co-adsorption of heavy metal ions and an organic pollutant by magnetic graphene nanomaterials in water. *Chemical Engineering Journal, 358*, 1399–1409.
Hummers, W. S., & Offeman, R. E. (1958). Preparation of graphitic oxide. *Journal of the American Chemical Society, 80*, 1339.
Iordache, M. L., Dodi, G., Hritcu, D., Draganescu, D., Chiscan, O., & Popa, M. I. (2018). Magnetic chitosan grafted (alkyl acrylate) composite particles: Synthesis, characterization and evaluation as adsorbents. *Arabian Journal of Chemistry, 11*, 1032–1043.
Jin, Z., Wang, X., Sun, Y., Ai, Y., & Wang, X. (2015). Adsorption of 4-nnonylphenol and bisphenol-A on magnetic reduced graphene oxides: A combined experimental and theoretical studies. *Environmental Science & Technology, 49*, 9168–9175.
Kaeseberg, T., Zhang, J., Schubert, S., Oertel, R., Siedel, H., & Krebs, P. (2018). Sewer sediment-bound antibiotics as a potential environmental risk: Adsorption and desorption affinity of 14 antibiotics and one metabolite. *Environmental Pollution, 239*, 638–647.
Kang, D. J., Yu, X. L., Ge, M. F., Xiao, F., & Xu, H. (2017). Novel Al-doped carbon nanotubes with adsorption and coagulation promotion for organic pollutant removal. *Journal of the Environmental Sciences, 54*, 1–12.
Lan, S., Leng, Z. H., Guo, N., Wu, X. M., & Gan, S. C. (2014). Sesbania gum-based magnetic carbonaceous nanocomposites: Facile fabrication and adsorption behavior. *Colloids and Surfaces A, Physicochemical and Engineering Aspects, 446*, 163–171.
Li, D. M., Zhang, B., & Xuan, F. Q. (2015). The sequestration of Sr(II) and Cs(I) from aqueous solutions by magnetic graphene oxides. *Journal of Molecular Liquids, 209*, 508–514.

Li, N., Jiang, H. L., Wang, X. L., Wang, X., Xu, G. J., Zhang, B. B., et al. (2018). Recent advances in graphene-based magnetic composites for magnetic solid-phase extraction. *TrAC Trends in Analytical Chemistry, 102*, 60–74.

Liu, F., Chung, S., Oh, G., & Seo, T. S. (2012). Three-dimensional graphene oxide nanostructure for fast and efficient water-soluble dye removal. *ACS Applied Materials & Interfaces, 4*, 922–927.

Liu, Y. S., Li, M., & He, C. Y. (2017). Removal of Cr(VI) and Hg(II) ions from wa stewater by novel β-CD/MGO-SO3H. *Colloids and Surfaces A, Physicochemical and Engineering Aspects, 512*, 129–136.

Nachiappan, S., & Gopinath, K. P. (2015). Treatment of pharmaceutical effluent using novel heterogeneous fly ash activated persulfate system. *Journal of Environmental Chemical Engineering, 3*, 2229–2235.

Naeimi, S., & Faghihian, H. (2018). Remediation of pharmaceutical contaminated water by use of magnetic functionalized metal organic framework. Physicochemical study of doxycycline adsorption. *Water and Environment Journal, 32*, 422–432.

Rafatullah, M., Sulaiman, O., Hashim, R., & Ahmad, A. (2010). Adsorption of methylene blue on low-cost adsorbents: A review. *Journal of Hazardous Materials, 177*, 70–80.

Reddy, D. H. K., & Yun, Y. S. (2016). Spinel ferrite magnetic adsorbents: Alternative future materials forwater purification. *Coordination Chemistry Reviews, 315*, 90–111.

Regti, A., Ayouchia, H. B. E., Laamari, M. R., Stiriba, S. E., Anane, H., & ElHaddad, M. (2016). Experimental and theoretical study using DFT method for the competitive adsorption of two cationic dyes from wastewaters. *Applied Surface Science, 390*, 311–319.

Sargin, I., Arslan, G., & Kaya, M. (2019). Production of magnetic chitinous microcages from ephippia of zooplankton Daphnia longispina and heavy metal removal studies. *Carbohydrate Polymers, 207*, 200–210.

Shah, J., Jan, M. R., & Tasmia (2018). Magnetic chitosan graphene oxide composite for solid phase extraction of phenylurea herbicides. *Carbohydrate Polymers, 199*, 461–472.

Su, H., Ye, Z. B., & Hmidi, N. (2017). High-performance iron oxide–graphene oxide nanocomposite adsorbents for arsenic removal. *Colloids and Surfaces A, Physicochemical and Engineering Aspects, 522*, 161–172.

Tabaraki, R., & Sadeghinejad, N. (2018). Comparison of magnetic Fe_3O_4/chitosan and arginine-modified magnetic Fe_3O_4/chitosan nanoparticles in simultaneous multidye removal: Experimental design and multicomponent analysis. *International Journal of Biological Macromolecules, 120*, 2313–2323.

Vadivelan, V., & Kumar, K. V. (2005). Equilibrium, kinetics, mechanism, and process design for the sorption of methylene blue onto rice husk. *Journal of Colloid and Interface Science, 286*, 90–100.

Wang, K. X., Ma, H., Pu, S. Y., Yan, C., Wang, M. T., Yu, J., et al. (2019). Hybrid porous magnetic bentonite-chitosan beads for selective removal of radioactive cesium in water. *Journal of Hazardous Materials, 362*, 160–169.

Wang, P., Shi, Q., Shi, Y., Clark, K. K., Stucky, G. D., & Keller, A. A. (2009). Magnetic permanently confined micelle arrays for treating hydrophobic organic compound contamination. *Journal of the American Chemical Society, 131*, 182–188.

Wen, Y., Ma, J., Chen, J., Shen, C., Li, H., & Liu, W. (2015). Carbonaceous sulfur-containing chitosan–Fe(III): A novel adsorbent for efficient removal of copper (II) from water. *Chemical Engineering Journal, 259*, 372–380.

Wu, Y., Yang, F., Liu, X. X., Tan, G. Q., & Xiao, D. (2018). Fabrication of N, P-codoped reduced graphene oxide and its application for organic dye removal. *Applied Surface Science, 435*, 281–289.

Xu, Y. X., Zhao, L., Bai, H., Hong, W. J., Li, C., & Shi, G. Q. (2009). Chemically converted graphene induced molecular flattening of 5,10,15,20-tetrakis (1-methyl-4-pyridinio) porphyrin and its application for optical detection of cadmium(II) ions. *Journal of the American Chemical Society, 131*, 13490–13497.

Yu, B. W., Bai, Y. T., Ming, Z., Yang, H., Chen, L. Y., Hu, X. J., et al. (2017). Adsorption behaviors of tetracycline on magnetic graphene oxide Sponge. *Materials Chemistry and Physics, 198*, 283–290.

Zhao, M. F., & Liu, P. (2009). Adsorption of methylene blue from aqueous solutions by modified expanded graphite powder. *Desalination, 249*, 331–336.